JOC Article
pubs.acs.org/joc

Synthesis of $(NH)_m(NMe)_{4-m}$-Bridged Calix[4]pyridines and the Effect of NH Bridge on Structure and Properties

En-Xuan Zhang,[†] De-Xian Wang,*[,†] Zhi-Tang Huang,[†] and Mei-Xiang Wang*[,†,‡]

[†]*Beijing National Laboratory for Molecular Sciences, CAS Key Laboratory of Molecular Recognition and Function, Institute of Chemistry, Chinese Academy of Sciences, Beijing 100190, China, and* [‡]*The Key Laboratory of Bioorganic Phosphorus Chemistry & Chemical Biology (Ministry of Education), Department of Chemistry, Tsinghua University, Beijing 100084, China*

mxwang@iccas.ac.cn; wangmx@mail.tsinghua.edu.cn

Received July 24, 2009

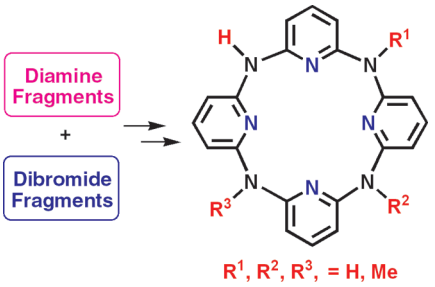

The $(NH)_m(NMe)_{4-m}$-bridged calix[4]pyridines (m = 1−4) **19**−**23** were synthesized in excellent yields from deprotection of *N*-allyl groups of $(NAllyl)_m(NMe)_{4-m}$-bridged calix[4]pyridine derivatives **8** and **15**−**18**, which were prepared in moderate yields by macrocyclic 2+2 and 1+3 coupling reactions between simple diamino- and dibromo-substituted fragments. In the solid state, $(NH)_m(NMe)_{4-m}$-bridged calix[4]pyridines adopted different 1,3-alternate conformations due to mainly the formation of varied conjugation systems of bridging NH units with their neighboring pyridines. In solution, all $(NH)_m(NMe)_{4-m}$-bridged calix[4]pyridines were very fluxional and the rates of interconversion of various conformational structures were very rapid relative to the NMR time scale. While $(NH)_4$-bridged calix[4]pyridine **23** formed the strongest conjugation system, $(NH)_2(NMe)_2$-bridged calix[4]pyridine **21** acted as a selective fluorescence probe in the recognition of zinc(II) ion in solution with the dramatic enhancement of fluorescence intensity.

Introduction

Heterocalixaromatics,[1−5] heteroatom-bridged calixaromatics, are an emerging generation of macrocyclic host molecules in supramolecular chemistry. Because the heteroatoms can adopt different electronic configurations and form various degrees of conjugation with their adjacent aromatic rings, the conformation and the cavity structures of the heterocalixaromatics are fine-tuned by the bond lengths and bond angles of the bridging heteroatoms. For example, by the formation of marginally different conjugations between the bridging nitrogen atoms and their neighboring pyridines, tetramethylazacalix[4]pyridine has been found to yield cavities of different sizes in order to interact with different guest species.[2e,f,l,o] In addition, the various electronic effects of the heteroatoms also influence the electron density of aromatic rings, producing the cavity of varied electronic features. The tetramethylazacalix[4]pyridines, for instance, are able to interact with many metal cations whereas the oxygen-bridged calix[2]arene[2]triazines complex halides through anion−π interactions.[6] Furthermore, the heterocalixaromatics are readily functionalized not only on the aromatic rings[7] but also on the bridging positions,[8] allowing the construction of polyfunctionalized host molecules.

A large number of heterocalixaromatics have been prepared via mainly the fragment coupling reactions and

*To whom correspondence should be addressed.

(1) For useful reviews of heterocalixaromatics, see: (a) Wang, M.-X. *Chem. Commun.* **2008**, 4541. (b) Maes, W.; Dehaen, W. *Chem. Soc. Rev.* **2008**, *37*, 2393. (c) Tsue, H.; Ishibashi, K.; Tamura, R. *Top. Heterocycl. Chem.* **2008**, *17*, 73. (d) König, B.; Fonseca, M. H. *Eur. J. Inorg. Chem.* **2000**, 2303.

DOI: 10.1021/jo901609u Published on Web 10/26/2009

one-pot reaction fashions starting from cheap and readily available (hetero)aromatic dinucleophilic and dielectrophilic reactants.[1] Surprisingly, however, NH-bridged calixaromatics still remain largely unexplored. For example, using the fragment coupling method, we[3a] previously prepared NH-bridged calix[2]arene[2]triazines from 1,3-phenylenediamine and cyanuric chloride. Siri[9] and Konishi[10] independently reported the synthesis of NH-bridged calix[4]arenes by reacting 1,3-phenylenediamine with 1,5-difluoro-2,4-dinitrobenzenes. The use of 1,3-dibromobenzenes as dielectrophiles in the reaction with 1,3-phenylenediamine led to none or very low yields of NH-bridged calixaromatics.[2h] Recently, Rajca and co-workers[11a] and Tsue and co-workers[11b,c] reported the synthesis of NH-bridged calix[*n*]arenes from exhaustive debenzylation of NBn-bridged calix[*n*]arenes.

For years, we have been interested in the heterocalix[*n*]-pyridine derivatives because of their intriguing cavity structures and versatile properties in recognizing various metal cations and neutral molecules.[1a] It is highly desirable to have the NH-bridged calix[*n*]pyridine derivatives in order to understand the substituent effect of the bridging nitrogen atoms on the structure and property of azacalix[*n*]pyridines. Very recently, combining the fragment coupling method and *N*-Boc protection/deprotection strategy, we have synthesized NH-bridged calix[*m*]arene[*n*]pyridines ($m = 1$, $n = 3$; $m = n = 2$).[12] The method, unfortunately, does not work for the synthesis of NH-bridged calix[4]pyridine. We report herein the efficient synthesis of a series of $(NH)_m(NMe)_{4-m}$-bridged calix[4]pyridines ($m = 1-4$) from 2+2 and 1+3 fragment coupling reactions followed by deallylation reaction. It has been found indeed that NH bridge(s) played an important role in determining the conformational structures and properties of the resulting macrocycles.

Results and Discussion

We started our study with the synthesis of $(NH)(NMe)_3$-bridged calix[4]pyridine. The strategy was based on the deprotection of the *N*-protection group of azacalix-[4]pyridine. We envisioned that the introduction of an allyl group on bridging nitrogen would afford the formation of $(NAllyl)(NMe)_3$-bridged calix[4]pyridine from the cross-coupling reaction between diamine fragment **4** and dibromide fragment **7**. Deprotection of the allyl group on bridging nitrogen of the resulting $(NAllyl)(NMe)_3$-bridged calix-[4]pyridine would then give the desired $(NH)(NMe)_3$-bridged calix[4]pyridine. Scheme 1 shows the preparation of fragments **4** and **7**. Nucleophilic substitution reaction of 2,6-dibromopyridine **1** with methylamine at 190 °C in an autoclave gave 6-bromo-2-methylaminopyridine **2** in 92% yield. Treatment of **2** with sodium hydride followed by 2,6-dibromopyridine produced dibromide intermediate **3** in 98% yield. Diamination of **3** with methylamine in an autoclave afforded product **4** in an almost quantitative yield. A similar monoamination reaction of **1** with ammonia in an autoclave gave 6-bromo-2-aminopyridine **5**, which underwent nucleophilic reaction with **1** in the presence of sodium hydride to afford bis(6-bromopyridin-2-yl)amine **6** in 88% yield. Reaction between **6** and allyl bromide with the aid of sodium hydride yielded *N*-allylbis(6-bromopyridin-2-yl)amine **7** almost quantitatively (Scheme 1).

We then investigated the macrocyclic cross-coupling reaction between **4** and **7** (Scheme 2). The effects of catalyst, ligand, base, reaction temperature, ratio between reactants, and concentration of reactants were examined (see Table S1 in the SI). It has been found that $Pd_2(dba)_3$ showed higher catalytic efficiency than $Pd(PPh)_4$, $PdCl_2(PPh)_2$, and $PdCl_2$ (entries 1−6, Table S1 in the SI). Bidentate ligand dppp was a better ligand than dppf, dppb, and $P(c\text{-Hex})_3$ (entries 6−10, Table S1 in the SI). While a polar solvent such as DMF, DMSO, and DME had a detrimental effect on the cross-coupling reaction, toluene turned out to be the best solvent

(2) For recent examples of nitrogen-bridged calixaromatics, see: (a) Ito, A.; Ono, Y.; Tanaka, K. *New J. Chem.* **1998**, 779. (b) Ito, A.; Ono, Y.; Tanaka, K. *J. Org. Chem.* **1999**, *64*, 8236. (c) Miyazaki; Kanbara, T.; Yamamoto, T *Tetrahedron Lett.* **2002**, *43*, 7945. (d) Wang, M.-X.; Zhang, X.-H.; Zheng, Q.-Y. *Angew. Chem., Int. Ed.* **2004**, *43*, 838. (e) Gong, H.-Y.; Zhang, X.-H.; Wang, D.-X.; Ma, H.-W.; Zheng, Q.-Y.; Wang, M.-X. *Chem.—Eur. J.* **2006**, *12*, 9262. (f) Gong, H.-Y.; Zheng, Q.-Y.; Zhang, X.-H.; Wang, D.-X.; Wang, M.-X. *Org. Lett.* **2006**, *8*, 4895. (g) Tsue, H.; Ishibashi, K.; Takahashi, H.; Tamura, R. *Org. Lett.* **2005**, *7*, 11. (h) Fukushima, W.; Kanbara, T.; Yamamoto, T. *Synlett* **2005**, *19*, 2931. (i) Selby, T. D.; Blackstock, S. C. *Org. Lett.* **1999**, *1*, 2053. (j) Suzuki, Y.; Yanagi, T.; Kanbara, T.; Yamamoto, T. *Synlett* **2005**, *2*, 263. (k) Ishibashi, K.; Tsue, H.; Tokita, S.; Matsui, K.; Takahashi, H.; Tamura, R. *Org. Lett.* **2006**, *8*, 5991. (l) Gong, H.-Y.; Wang, D.-X.; Xiang, J.-F.; Zheng, Q.-Y.; Wang, M.-X. *Chem.—Eur. J.* **2007**, *13*, 7791. (m) Liu, S.-Q.; Wang, D.-X.; Zheng, Q.-Y.; Wang, M.-X. *Chem. Commun.* **2007**, 3856. (n) Zhang, E.-X.; Wang, D.-X.; Zheng, Q.-Y.; Wang, M.-X. *Org. Lett.* **2008**, *10*, 2565. (o) Gong, H.-Y.; Wang, D.-X.; Zheng, Q.-Y.; Wang, M.-X. *Tetrahedron* **2009**, *65*, 87.

(3) For recent examples of oxygen-bridged calixaromatics, see: (a) Wang, M.-X.; Yang, H.-B. *J. Am. Chem. Soc.* **2004**, *126*, 15412. (b) Katz, J. L.; Feldman, M. B.; Conry, R. R. *Org. Lett.* **2005**, *7*, 91. (c) Katz, J. L.; Selby, K. J.; Conry, R. R. *Org. Lett.* **2005**, *7*, 3505. (d) Katz, J. L.; Geller, B. J.; Conry, R. R. *Org. Lett.* **2006**, *8*, 2755. (e) Maes, W.; Van Rossom, W.; Van Hecke, K.; Van Meervelt, L.; Dehaen, W. *Org. Lett.* **2006**, *8*, 4161. (f) Hao, E.; Fronczek, F. R.; Vicente, M. G. H. *J. Org. Chem.* **2006**, *71*, 1233. (g) Chambers, R. D.; Hoskin, P. R.; Kenwright, A. R.; Khalil, A.; Richmond, P.; Sandford, G.; Yufit, D. S.; Howard, J. A. K. *Org. Biomol. Chem.* **2003**, 2137. (h) Chambers, R. D.; Hoskin, P. R.; Khalil, A.; Richmond, P.; Sandford, G.; Yufit, D. S.; Howard, J. A. K. *J. Fluorine Chem.* **2002**, *116*, 19. (i) Li, X. H.; Upton, T. G.; Gibb, C. L. D.; Gibb, B. C. *J. Am. Chem. Soc.* **2003**, *125*, 650. (j) Yang, F.; Yan, L.-W.; Ma, K.-Y.; Yang, L.; Li, J.-H.; Chen, L.-J.; You, J.-S. *Eur. J. Org. Chem.* **2006**, 1109. (k) Wang, Q.-Q.; Wang, D.-X.; Zheng, Q.-Y.; Wang, M.-X. *Org. Lett.* **2007**, *9*, 2847. (l) Katz, J. L.; Geller, B. J.; Foster, P. D. *Chem. Commun.* **2007**, 1026. (m) Zhang, C.; Chen, C.-F. *J. Org. Chem.* **2007**, *72*, 3880. (n) Van Rossom, W.; Maes, W.; Kishore, L.; Ovaere, M.; Van Meervelt, L.; Dehaen, W. *Org. Lett.* **2008**, *10*, 585.

(4) For review on thiacalixarenes, see: Morohashi, N.; Narumi, F.; Iki, N.; Hattori, T.; Miyano, S. *Chem. Rev.* **2006**, *106*, 5291.

(5) For examples of other heteroatom-bridged calixaromatics, see: (a) König, B.; Rödel, M.; Bubenitschek, P.; Jones, P. G.; Thondorf, I. *J. Org. Chem.* **1995**, *60*, 7406. (b) König, B.; Rödel, M.; Bubenitschek, P.; Jones, P. G. *Angew. Chem., Int. Ed.* **1995**, *34*, 661. (c) Yoshida, M.; Goto, M.; Nakanishi, F. *Organometallics* **1999**, *18*, 1465. (d) Avarvari, N.; Mezailles, N.; Ricard, L.; Le Floch, P.; Mathey, F. *Science* **1998**, *280*, 1587. (e) Avarvari, N.; Maigrot, N.; Ricard, L.; Mathey, F.; Le Floch, P. *Chem.—Eur. J.* **1999**, *5*, 2109.

(6) Wang, D.-X.; Zheng, Q.-Y.; Wang, Q.-Q.; Wang, M.-X. *Angew. Chem., Int. Ed.* **2008**, *47*, 7485.

(7) (a) Yang, H.-B.; Wang, D.-X.; Wang, Q.-Q.; Wang, M.-X. *J. Org. Chem.* **2007**, *72*, 3757. (b) Hou, B.-Y.; Wang, D.-X.; Yang, H.-B.; Zheng, Q.-Y.; Wang, M.-X. *J. Org. Chem.* **2007**, *72*, 5218. (c) Hou, B.-Y.; Zheng, Q.-Y.; Wang, D.-X.; Wang, M.-X. *Tetrahedron* **2007**, *63*, 10801. (d) Hou, B.-Y.; Zheng, Q.-Y.; Wang, D.-X.; Huang, Z.-T.; Wang, M.-X. *Chem. Commun.* **2008**, 3864. (e) Yao, B.; Wang, D.-X.; Huang, Z.-T.; Wang, M.-X. *Chem. Commun.* **2009**, 2899.

(8) The N-arylation of NH-bridged calix[2]arene[2]triazine was reported: Wang, Q.-Q.; Wang, D.-X.; Ma, H.-W.; Wang, M.-X. *Org. Lett.* **2006**, *8*, 5967.

(9) Touil, M.; Lachkar, M.; Siri, O. *Tetrahedron Lett.* **2008**, *49*, 7250.

(10) Konishi, H.; Hashimoto, S.; Sakakibara, T.; Matsubara, S.; Yasukawa, Y.; Morikawa, O.; Kobayashi, K. *Tetrahedron Lett.* **2009**, *50*, 620.

(11) (a) Vale, M.; Pink, M.; Rajca, S.; Rajca, A. *J. Org. Chem.* **2008**, *73*, 27. (b) Tsue, H.; Ishibashi, K.; Tokita, S.; Takahashi, H.; Matsui, K.; Tamura, R. *Chem.—Eur. J.* **2008**, *14*, 6125. (c) Tsue, H.; Matsui, K.; Ishibashi, K.; Takahashi, H.; Tokita, S.; Ono, K.; Tamura, R. *J. Org. Chem.* **2008**, *73*, 7748.

(12) Yao, B.; Wang, D.-X.; Gong, H.-Y.; Huang, Z.-T.; Wang, M.-X. *J. Org. Chem.* **2009**, *74*, 5361.

SCHEME 1. Preparation of Fragments 4 and 7

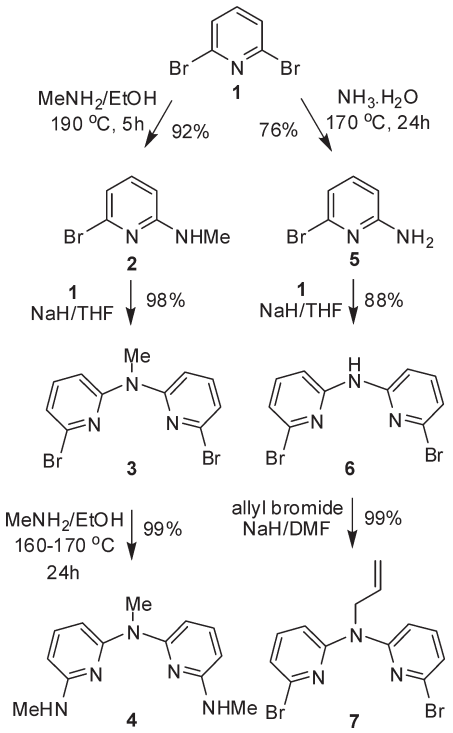

(entries 6 and 11−14, Table S1 in the SI). It was noteworthy that $NaOBu^t$ worked well for the cross-coupling reaction whereas other bases such as $LiOBu^t$, $KOBu^t$, Cs_2CO_3, and NaH did not effect the formation of macrocyclic products (entries 14−18, Table S1 in the SI). The use of a slight excess amount of dibromide fragment **4** was beneficial for the macrocyclic cross-coupling reaction between **4** and **7** (entries 14 and 19−22, Table S1 in the SI). It was worth noting that the reaction between **4** and **7** (**4**:**7** = 1.1:1) at a concentration of 5 mM in refluxing toluene gave desired (NAllyl)$(NMe)_3$-bridged calix[4]pyridine **8** in 36% yield. Either lower reaction temperature (entries 14 and 23−25, Table S1 in the SI) or varied concentrations (entries 14 and 26−29, Table S1 in the SI) of the reactants led to the decrease of chemical yield of product **8**. In addition to the targeted product **8**, the cross-coupling reaction between **4** and **7** also gave *N*-propenyl-bridged azacalixpyridine **8′** (*E*:*Z* = 2.5:1), an isomer of **8** with the shift of the carbon−carbon double bond (Scheme 2). Interestingly, the formation of **8** and **8′** was governed by the amount of catalyst and ligand used. As summarized in Table 1, the decrease of catalyst loading led to the increase of product **8′**. When 2.5 mol % of $Pd_2(dba)_3$ was employed, *N*-propenyl-bridged azacalix[4]pyridine **8′** was obtained as the major product in 30% yield (entry 6, Table 1). Longer reaction time led to the isomerization of the carbon−carbon double bond (entries 4 and 5, Table 1). The amount of $NaOBu^t$ used appeared critical in terms of the chemical yield and the ratio of the products. The reaction proceeded less efficiently when 2 equiv of $NaOBu^t$ were applied (entries 3 and 8, Table 1). The use of more than 4 equiv of $NaOBu^t$ gave *N*-propenyl-bridged azacalix[4]pyridine **8′** in a lower chemical yield (entries 9−11, Table 1).

TABLE 1. Macrocyclic Cross-Coupling Reaction between 4 and 7[a]

entry	$Pd_2(dba)_3$ (mol %)	dppp (mol %)	$NaOBu^t$ (equiv)	time (h)	**8** (%)[b]	**8′** (%)[b]
1	20	40	3	5	31	
2	15	30	3	5	36	
3	10	20	3	5	36	
4	5	10	3	5	31	
5	5	10	3	24	31	4.8
6	2.5	5	3	5	3	30
7	2.5	5	3	24	5	21
8	10	20	2	6	15	
9	10	20	4	5	26	8
10	10	20	5	5		28
11	10	20	6	5		28

[a]The ratio of **4** over **7** was 1.1:1, and the concentration of reactants was 5 mM. [b]Isolated yield.

Encouraged by the synthesis of (NAllyl)$(NMe)_3$-bridged calix[4]pyridine **8** from the Pd-catalyzed macrocyclic cross-coupling reaction between diamine fragment **4** and dibromide fragment **7**, we then attempted the synthesis of other (NAllyl)$_m$(NMe)$_{4-m}$-bridged calix[4]pyridines (m = 2−4). The preparation of necessary fragments was illustrated in Schemes 3 and 4. 2,6-Bis(methylamino)pyridine **9** and 2,6-bis(allylamino)pyridine **11**, which were obtained respectively from diamination of 2,6-dibromopyridine **1** with methylamine and allylamine, underwent nucleophilic aromatic substitution reaction with 2,6-dibromopyridine **1** in the presence of sodium hydride to afford the corresponding linear trimers **10** and **12** (Scheme 3). The nucleophilic substitution reaction of **7** with methylamine at high temperature gave *N*-allylbis(6-methylaminopyridin-2-yl)amine **13** in 78% yield while CuI/L-proline-catalyzed cross-coupling reaction between 6-bromo-2-methylaminopyridine **2** and allylamine resulted in the formation of 2-allylamino-6-methylaminopyridine **14** in 67% yield (Scheme 4).

SCHEME 2. Macrocyclic Cross-Coupling Reaction between 4 and 7

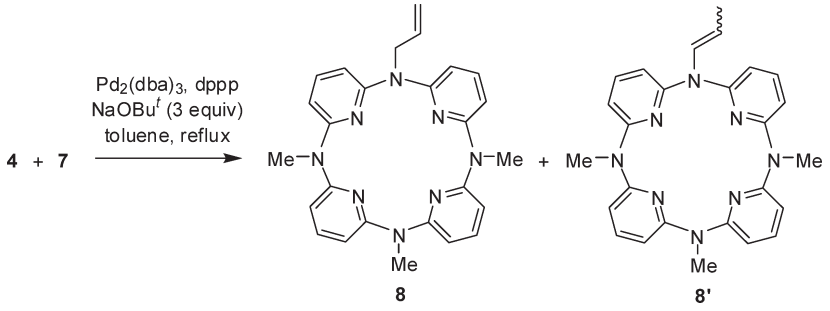

SCHEME 3. Preparation of Fragments 10−12

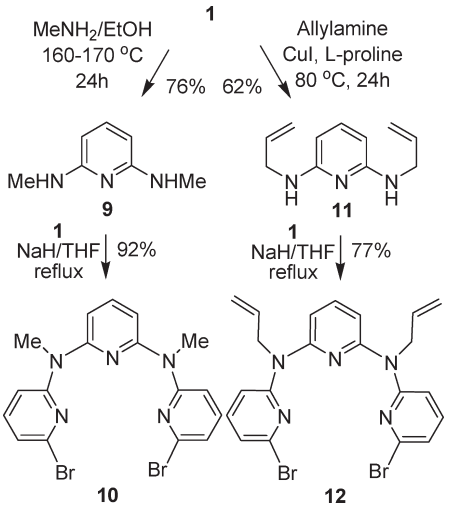

SCHEME 4. Preparation of Fragments 13 and 14

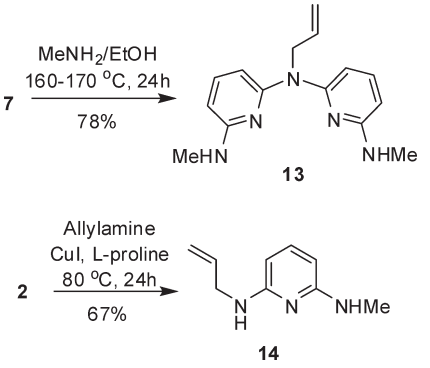

SCHEME 5. Synthesis of Azacalix[4]pyridine 15

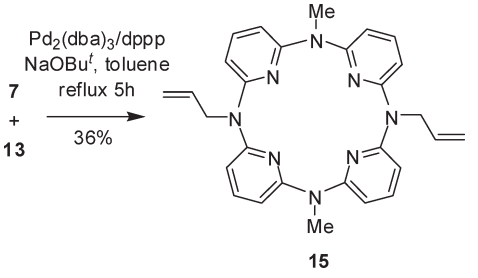

Under the optimized conditions for the synthesis of (NAllyl)(NMe)$_3$-bridged calix[4]pyridine **8** (entry 3, Table 1), the 2+2 fragment coupling reaction between *N*-allylbis(6-bromopyridin-2-yl)amine **7** and *N*-allylbis(6-methylaminopyridin-2-yl)amine **13** afforded (NAllyl)$_2$(NMe)$_2$-bridged calix[4]pyridine **15** in 36% yield (Scheme 5). The method was also successfully applied for the synthesis of other (NAllyl)$_m$(NMe)$_{4-m}$-bridged calix[4]pyridines **16**−**18** (Scheme 6). For example, the Pd-catalyzed macrocyclic cross coupling of a linear trimer **10** with 2,6-bis(allylamino)pyridine **11** gave rise to the formation of (NAllyl)$_2$(NMe)$_2$-bridged calix[4]pyridine **16** in 36% yield. (NAllyl)$_3$(NMe)-bridged calix[4]pyridine **17** and (NAllyl)$_4$-bridged calix[4]pyridine **18** were synthesized respectively from the 1+3 fragment coupling reaction of reactant **12** with 2-allylamino-6-methylaminopyridine **14** and with 2,6-bis(allylamino)pyridine **11** (Scheme 6).

SCHEME 6. Synthesis of Azacalix[4]pyridines 16−18

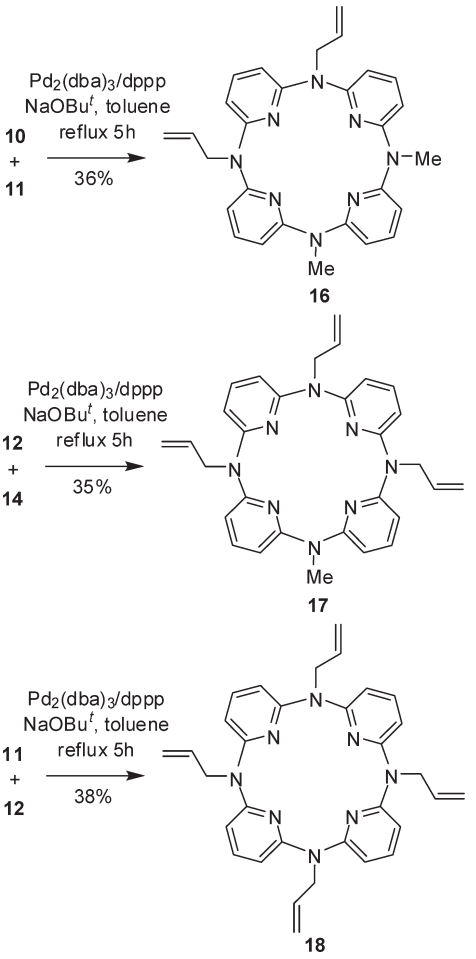

To obtain (NH)$_m$(NMe)$_{4-m}$-bridged calix[4]pyridines (m = 1−4), the cleavage of allyl groups from the bridging nitrogen atoms of azacalix[4]pyridines **8** and **15**−**18** was performed under alkaline condition followed by acidic hydrolysis.[13] When treated with KOBu^t at 100 °C in DMSO, the allyl group underwent isomerization of the carbon−carbon double bond to form an enamine intermediate such as **8′**. The subsequent hydrolysis under acidic conditions furnished desired (NH)$_m$(NMe)$_{4-m}$-bridged calix[4]pyridines (m = 1−4) **19**−**23** in the yield ranging from 96% to 100% (Scheme 7).

All (NH)$_m$(NMe)$_{4-m}$-bridged calix[4]pyridine (m = 1−4) products **19**−**23** were crystalline products and they gave high-quality single crystals suitable for X-ray diffraction analysis (Table S2 in the SI). The X-ray crystal structures revealed that introduction of NH linkage into the bridging positions of calix[4]pyridines led to interesting conformational structures in the solid state. We[2f,o] have previously shown that (NMe)$_4$-bridged calix[4]pyridine adopts a highly symmetric 1,3-alternate conformation in the solid state. All bridging nitrogen atoms, which adopt sp^2 electronic configuration, form conjugation with one of their adjacent pyridine rings. The cavity of (NMe)$_4$-bridged calix[4]pyridine is

(13) Gigg, R.; Conant, R. *J. Carbohydr. Chem.* **1983**, *1*, 331.

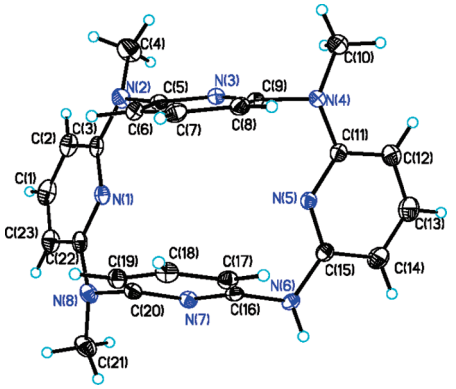

FIGURE 1. X-ray crystal structure of $(NH)(NMe)_3$-bridged calix[4] pyridine **19** (top view). Selected bond lengths [Å]: N(2)−C(3) 1.377(2); N(2)−C(5) 1.431(2); N(4)−C(11) 1.394(2); N(4)−C(9) 1.437(2); N(6)−C(15) 1.394(2); N(6)−C(16) 1.411(2); N(8)−C(22) 1.395(2); N(8)−C(20) 1.434(2). Selected interatomic distances [Å]: C(3)−C(13) 8.970; C(7)−C(18) 3.341.

SCHEME 7. Synthesis of $(NH)_m(NMe)_{4-m}$-Bridged Calix-[4]pyridines 19−23

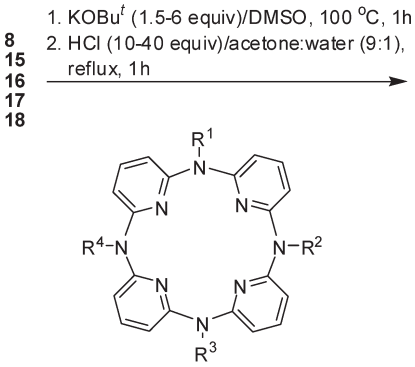

19 R^1 = H, R^2 = R^3 = R^4 = Me, 96%
20 R^1 = R^3 = H, R^2 = R^4 = Me, 100%
21 R^1 = R^2 = H, R^3 = R^4 = Me, 100%
22 R^1 = R^2 = R^3 = H, R^4 = Me, 96%
23 R^1 = R^2 = R^3 = R^4 = H, 98%

composed of two conjugated planar segments 2,6-bis-(methylamino)pyridine (NMe-Py-NMe) and two isolated pyridine (-Py-) segments in a 1,3-alternate fashion. With one NH bridge, $(NH)(NMe)_3$-bridged calix[4]pyridine **19** almost remained in the same 1,3-alternate conformation as $(NMe)_4$-bridged calix[4]pyridine, with two isolated pyridine rings being face-to-face paralleled while conjugated pyridine units NH-Py-NMe and NMe-Py-NMe tended to be edge-to-edge orientated (Figure 1, as well as Figure S1 in the SI). Although the slightly twisted 1,3-alternate conformation was observed for $(NH)_2(NMe)_2$-bridged calix[4]pyridine **20** (Figure S2 in the SI), the bond lengths between bridging nitrogen atoms and carbon atoms of pyridine rings indicated that two of the pyridine rings formed conjugation with both NH and NMe linkages while the other two pyridine rings did not conjugate with any bridging heteroatoms. As an isomer of **20**, both discrete $(NH)_2(NMe)_2$-bridged calix[4]pyridine molecules **21** in a cell unit gave similar heavily twisted 1,3-alternate conformational structures (Figure S3 in the SI). However, the conjugations between bridging nitrogen atoms with their neighboring pyridine rings were different from

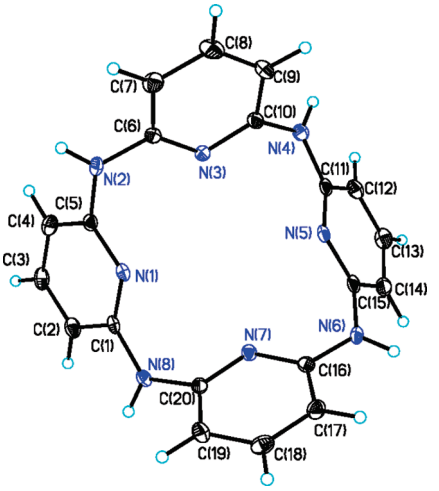

FIGURE 2. X-ray crystal structure of $(NH)_4$-bridged calix-[4]pyridine **23** (top view). Solvent molecules were not shown for clarity. Selected bond lengths [Å]: N(2)−C(6) 1.391(4); N(2)−C(5) 1.397(4); N(4)−C(11) 1.377(4); N(4)−C(10) 1.402(4); N(6)−C(16) 1.373(4); N(6)−C(15) 1.407(4); N(8)−C(1) 1.379(4); N(8)−C(20) 1.421(4). Selected interatomic distances [Å]: C(3)−C(13) 7.798; C(8)−C(18) 7.922.

that in macrocycle **20**. As indicated by bond lengths of linking nitrogen units, the cavity of **21** resulted from two conjugated aminopyridine and two methylaminopyridine segments in a 1,3-alternate cyclic array. Both $(NH)_3(NMe)$- and $(NH)_4$-bridged calix[4]pyridines **22** and **23** showed twisted 1,3-alternate conformations in the solid state, with each bridging nitrogen atom forming conjugation with one of its pyridine rings attached (Figure S4 (SI), as well as and Figure 2 and in the SI Figure S5). It was also interesting to point out that the cavity size of azacalix[4]pyridines **19**−**23** varied with the number of NH linkages in macrocycles. For instance, the upper rim distance between two face-to-face paralleled pyridines ranged from 3.341 (**19**), 3.524 (**20**), 7.729−7.883 (**21**), 7.980 (**23**) to 8.030 (**22**), while the distance between edge-to-edge orientated pyridines changed from 8.970 (**19**), 8.853 (**20**), 7.992 (**23**), 8.053−9.022 (**21**) to 8.519 (**22**) (see the captions in Figures 1 and 2, as well as Figures S2−S4 in the SI).

The molecular assemblies of $(NH)_m(NMe)_{4-m}$-bridged calix[4]pyridines **19**−**23** in the solid state were also worth addressing. Being different from $(NMe)_4$-bridged calix-[4]pyridine, NH linkages in $(NH)_m(NMe)_{4-m}$-bridged calix-[4]pyridines **19**−**23** were able to form different types of intermolecular hydrogen bonds and hydrogen bonds with solvent molecules. In addition, other noncovalent interactions such as π/π interactions and C−H/π also played a part in directing the molecular assembly. $(NH)(NMe)_3$-bridged calix[4]pyridine **19**, for example, formed a pair of intermolecular hydrogen bonds by its -NH-Py- moiety, yielding a dimeric structure (Figure S6 in the SI). A dimeric structure of $(NH)_2(NMe)_2$-bridged calix[4]pyridine **20** was also observed in the crystal structure. In addition to a pair of intermolecular hydrogen bonds, $\pi-\pi$ interaction between two pyridine rings from different molecules also contributed to the formation of the dimer (Figure S7 in the SI). In the case of compounds **21**−**23**, no hydrogen bond formed between macrocyclic molecules. Instead, they were assembled via

TABLE 2. Spectroscopic Properties of $(NH)_m(NMe)_{4-m}$-Bridged Calix[4]pyridines 19−23

entry	compd	λ_{max} (nm)[a]	ε ($cm^{-1}M^{-1}$) [a]	λ_{ex} (nm)[b]	λ_{em} (nm) [b]	Φ_f (%) [b,c]	$\Phi_{f(zinc)}$ (%)[b,c]	E_1^{ox} (V)[d]
1	**19**	309	2.03×10^4	324	404	1.99	4.33	0.430
2	**20**	307	2.26×10^4	314	372	2.63	4.10	0.464
3	**21**	308	2.20×10^4	327	392	0.58	7.63	0.446
4	**22**	314	2.43×10^4	320	398	3.25	7.42	0.392
5	**23**	316	3.30×10^4	332	412	1.70	4.37	0.348

[a]UV−vis spectra were measured in methanol solution (2.0×10^{-5} M) at 298 K. [b]Fluorescence emission spectra were measured in methanol solution (1.0×10^{-5} M) at 298 K. [c]Quinine sulfate was used as a standard. [d]Cyclic voltametric curves were measured at 298 K in acetonitrile containing 0.1 M Bu_4NClO_4 as the supporting electrolyte. Concentrations of **19**−**23** were 0.975, 1.010×10^{-3}, 1.010×10^{-3}, 0.523×10^{-3}, and 0.543×10^{-3} M, respectively.

the hydrogen bonds with water and methanol molecules (Figures S8−S10 in the SI). It was interesting to note that one of the clefts of $(NH)_2(NMe)_2$-bridged calix[4]pyridine **21** interacted with two water molecules (Figure S8 in the SI). More interestingly, while each of two clefts of $(NH)_4$-bridged calix[4]pyridine **23** accommodated one methanol molecule by hydrogen bonding and C−H/π interaction (Figure S10 in the SI), two clefts of $(NH)_3$(NMe)-bridged calix[4]pyridine **22** bonded different guest species such as a water molecule and a methanol molecule. The C−H/π interaction was also evidenced in the latter case (Figure S9 in the SI).

Although in the solid state $(NH)_m(NMe)_{4-m}$-bridged calix[4]pyridine (m = 1−4) products **19**−**23** existed in certain conformations with different conjugation systems being observed, these macrocycles might not be able to retain these stable conformational structures in the solution. In both ^{1}H and ^{13}C NMR spectra, only one set of proton and carbon resonance signals was observed for $(NH)_m(NMe)_{4-m}$-bridged calix[4]pyridines (m = 1−4). For example, $(NH)_4$-bridged calix[4]pyridine **23** gave a pair of coupled triplet and doublet peaks of the protons of 2,6-disubstituted pyridine rings, whereas only one singlet peak corresponding to two *N*-Me groups was observed for **20** and **21**. In the case of **19**, two singlet peaks at 3.20 (6H) and 3.19 ppm (3H) were found. These NMR spectral characteristics indicated that all $(NH)_m(NMe)_{4-m}$-bridged calix[4]pyridine (m = 1−4) products **19**−**23** might adopt highly symmetric conformational structures in solution. Most probably, these macrocycles were very fluxional in solution, and the rates of interconversion of various conformational structures might be very rapid relative to the NMR time scale. The high conformational mobility of these $(NH)_m(NMe)_{4-m}$-bridged calix[4]pyridines (m = 1−4) was most likely due to the lack of steric hindrance and intramolecular hydrogen bonds, both being key factors in stabilizing conformational structures of conventional calix[*n*]arenes in solution. The stability gained from the conjugation effect of the linking nitrogen atoms with their adjacent aromatic rings seemed insufficient to prevent the rotation of aromatic rings around the meta−meta axes or through the annulus.[1,11]

To further understand the properties of $(NH)_m(NMe)_{4-m}$-bridged calix[4]pyridines (m = 1−4), UV−vis absorption spectra, fluorescence spectra, quantum efficiencies, and cyclic voltammetric curves of products **19**−**23** were measured (see Figures S11−S13 in the SI) and physicochemical data were summarized in Table 2. All $(NH)_m(NMe)_{4-m}$-bridged calix[4]pyridines (m = 1−4) gave a strong absorption band ($\varepsilon > 10^4$ cm^{-1} M^{-1}) around 312 nm in UV−vis absorption spectra. Noticeably, with the increase of NH bridges, the wavelength of the maximum absorption band of macrocycles increased slightly from 307 to 308 (**19**−**21**), to 314 (**22**), and to 316 nm (**23**) (entries 1−5, Table 2). Under irradiation, $(NH)_m(NMe)_{4-m}$-bridged calix[4]pyridines (m = 1−4) gave an emission band. The wavelength and quantum efficiency were, however, dependent upon the structure of azacalix[4]pyridines. For example, except for $(NH)(NMe)_3$-bridged calix[4]pyridine **19** that showed an emission band at 404 nm, the increase of NH bridges led to bathochromic shift of emission band from 372 (**20**) to 412 nm (**23**). The quantum efficiencies varied from 0.58% to 3.25%. The longest absorption band and the lowest first oxidation potential implied most probably that $(NH)_4$-bridged calix[4]pyridine **23** gave the strongest conjugation system in solution among all azacalix[4]pyridines prepared. The tendency of $(NH)_4$-bridged calix[4]pyridine **23** to form the strongest conjugation system compared to its analogues was most likely attributable to the least steric effect of bridging NH units.

Being multi-nitrogen-containing macrocycles, azacalix[4]pyridines acted as macrocyclic host molecules to interact with metal ions. It was interesting to note that all $(NH)_m(NMe)_{4-m}$-bridged calix[4]pyridine products (m = 1−4), similar to $(NMe)_4$-bridged calix[4]pyridine, gave an enhanced fluorescence emission band when they were interacted with zinc(II) ion (see Figures S12 in the SI). The magnitude of augmentation of fluorescence intensity was, however, governed by the structure of $(NH)_m(NMe)_{4-m}$-bridged calix[4]pyridines. While most of the macrocycles doubled their fluorescence intensity upon interaction with zinc(II) ion (entries 1, 2, 4, and 5, Table 2), for instance, a remarkable and more than 13-fold enhancement of fluorescence intensity was observed for $(NH)_2(NMe)_2$-bridged calix[4]pyridine **21** (entry 3, Table 2). The structure of $(NH)_m(NMe)_{4-m}$-bridged calix[4]pyridines was also found to play an important role in selective binding. On the basis of the fluorescence titration, all $(NH)_m(NMe)_{4-m}$-bridged calix[4]pyridines **19**−**23** formed 1:1 complex with zinc(II) ion. The binding constants (log K)[14] varied, however, from 6.4 (**23**), 6.7 (**22**), 7.1 (**19**), 7.3 (**20**), to 7.4 (**21**). More intriguingly, while azacalix[4]pyridines **20**, **22**, and **23** were able to bind copper(II) and mercury(II) ions and the binding constants (log K), which were obtained from the quench of fluorescence of the macrocyclic host molecules by metal ions (see Table S3 and Figures S14−S28 in the SI), ranged from 3.9 to 7.0, no interaction was observed at all between $(NH)(NMe)_3$-calix[4]pyridine **19**, $(NH)_2(NMe)_2$-bridged calix[4]pyridine **21**, and copper(II) and mercury(II) ions.

(14) (a) Gans, P.; Sabatini, A.; Vacca, A. *Talanta* **1996**, *43*, 1739. (b) Hyperquad2003 software, Protonic Software, http://www.hyperquad.co.uk

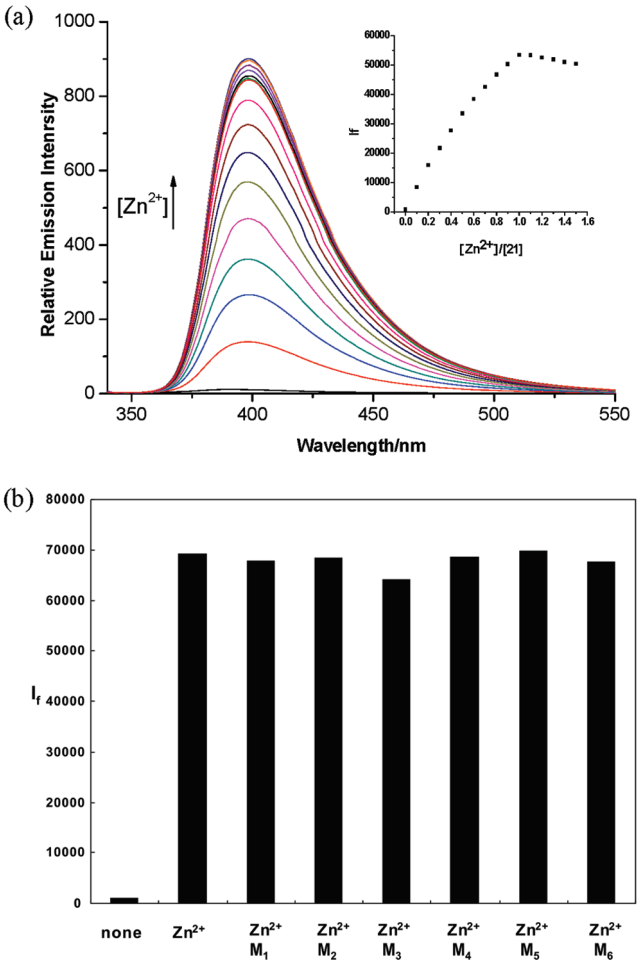

FIGURE 3. (a) Fluorescence titration of **21** by Zn^{2+} in methanol (1.0×10^{-5} M) at 298 K. The concentrations of Zn^{2+} for curves bottom to top were 0, 1.0×10^{-6}, 2.0×10^{-6}, 3.0×10^{-6}, 4.0×10^{-6}, 5.0×10^{-6}, 6.0×10^{-6}, 7.0×10^{-6}, 8.0×10^{-6}, 9.0×10^{-6}, 10.0×10^{-6}, 11.0×10^{-6}, 12.0×10^{-6}, 13.0×10^{-6}, 14.0×10^{-6}, 15.0×10^{-6} M. Inset: Variation of emission intensity from 340 to 550 nm of **21** with increasing Zn^{2+} concentration. (b) Emission intensity of **21** in response to various metal ions. Concentrations: **21**, 10 μM ; Zn^{2+}, 10 μM; M_1 (Na^+, K^+, NH_4^+, Ag^+), 100 μM (each); M_2 (Mg^{2+}, Ca^{2+}, Sr^{2+}, Ba^{2+}), 100 μM (each); M_3 (Mn^{2+}, Fe^{2+}, Co^{2+}, Ni^{2+}, Cu^{2+}), 100 μM (each); M_4 (Cd^{2+}, Hg^{2+}, Pb^{2+}), 100 μM (each); M_5 (Na^+, K^+, NH_4^+, Ag^+, Mg^{2+}, Ca^{2+}, Sr^{2+}, Ba^{2+}, Mn^{2+}, Fe^{2+}, Co^{2+}, Ni^{2+}, Cu^{2+}, Cd^{2+}, Hg^{2+}, Pb^{2+}), 100 μM (each); M_6 (Na^+, K^+, NH_4^+, Ag^+, Mg^{2+}, Ca^{2+}, Sr^{2+}, Ba^{2+}, Mn^{2+}, Fe^{2+}, Co^{2+}, Ni^{2+}, Cu^{2+}, Cd^{2+}, Hg^{2+}, Pb^{2+}), 200 μM (each). Metal perchlorate salts were used in all cases. λ_{ex} = 327 nm, and the excitation and emission band widths were 10 nm.

The sharp contrast between isomeric $(NH)_2(NMe)_2$-bridged calix[4]pyridines **20** and **21** in selectivity indicated that even the arrangement of two NH bridges could lead to a dramatic difference in molecular recognition. The significant fluorescence enhancement and high selectivity rendered $(NH)_2$-$(NMe)_2$-bridged calix[4]pyridine **21** an interesting fluorescence probe in the detection of zinc(II) ion. Figure 3 illustrates that the fluorescence titration of **21** by zinc(II) ion was not affected by the presence of other competing metal ion species including Na^+, K^+, NH_4^+, Ag^+, Mg^{2+}, Ca^{2+}, Sr^{2+}, Ba^{2+}, Mn^{2+}, Fe^{2+}, Co^{2+}, Ni^{2+}, Cu^{2+}, Cd^{2+}, Hg^{2+}, and Pb^{2+}.

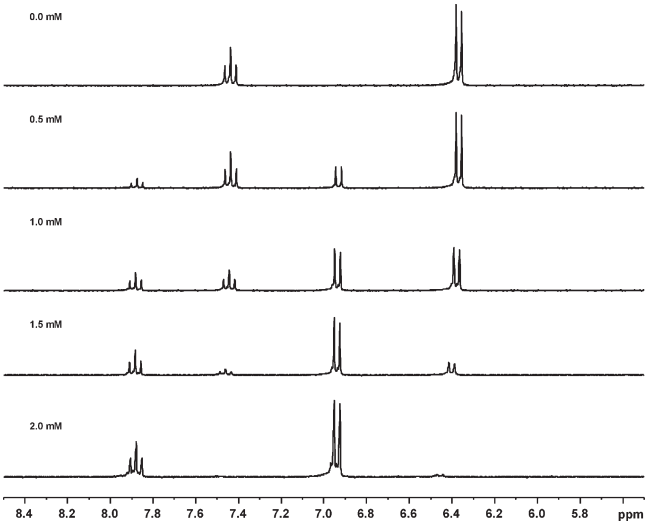

FIGURE 4. ^{1}H NMR spectra of **23** (2 mM) in CD_3OD in the absence and presence of $Zn(ClO_4)_2$ at 298 K.

The formation of 1:1 complex between $(NH)_m(NMe)_{4-m}$-bridged calix[4]pyridines and zinc(II) ion was further studied by ^{1}H NMR titration. As compiled in Figure 4, addition of $Zn(ClO_4)_2$ to the solution of **23** (2.0 mM)) in CD_3OD at 298 K led to the appearance of a new set of coupled triplet and doublet signals at 7.88 and 6.94 ppm, respectively, indicating a slow exchange process for the complexation of host with guest. Proton signals corresponding to the parent macrocycle disappeared after an equimolar amount of Zn-$(ClO_4)_2$ was added, and only a pair of downfield shifted triplet and doublet signals was observed. The downfield shift of the signals of pyridine protons was in agreement with the complexation of pyridine nitrogen with zinc(II) ion.

Last but not least, to reveal the complex structure between $(NH)_m(NMe)_{4-m}$-bridged calix[4]pyridines and metal ions, a high-quality single crystal of [**23**-Zn][ClO_4]$_2$ was cultivated and its X-ray molecular structure was obtained (Table S2 in the SI). As depicted in Figure 5, $(NH)_4$-bridged calix[4]-pyridine **23** acted as a tetradentate ligand. Four pyridine rings coordinated to zinc(II) ion, yielding a 1:1 square planar **23**-Zn^{2+} complex. The mean distance between pyridine nitrogen and zinc(II) ion was 2.098 Å. No binding between the bridging NH units and metal center was observed. In the axial positions, two water molecules coordinated to Zn(II) with the Zn−O distance being 2.154 and 2.219 Å, respectively. It was important to point out that the macrocyclic ring of the host molecule in the complex adopted a saddle conformation with an approximate S_4 symmetry, a conformation differed from its parent structure (see Figure 2). As exemplified by the bond lengths (see the caption for Figure 5), all bridging nitrogen atoms formed nearly the same conjugation with both of their neighboring pyridine rings. The outcomes suggested that the macrocyclic host molecules readily change their own conformational structure in order to complex with metal ion species. In other words, the presence of a metal ion species like zinc(II) ion might induce the macrocyclic host molecule to regulate its conformation, which could best fit the guest species. Nevertheless, it was the intrinsic nature of nitrogen bridges that self-tune their conjugation states with their linking pyridine rings, leading to

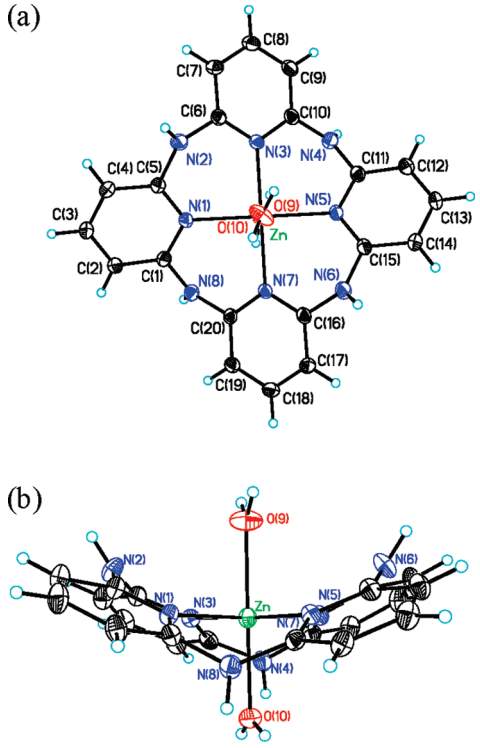

FIGURE 5. X-ray crystal structure of the complex between $(NH)_4$-bridged calix[4] pyridine **23** and $Zn(ClO_4)_2$: (a) top view and (b) side view. Anions were omitted for clarity. Selected bond lengths [Å]: N(2)−C(6) 1.392(5); N(2)−C(5) 1.392(5); N(4)−C(10) 1.393(5); N(4)−C(11) 1.395(5); N(6)−C(16) 1.393(5); N(6)−C(15) 1.393(5); N(8)−C(20) 1.397(5); N(8)−C(1) 1.399(5). Selected interatomic distances [Å]: Zn−N(1) 2.101(3); Zn−N(3) 2.094(3); Zn−N(5) 2.105(3); Zn−N(7) 2.094(3); Zn−O(9) 2.154(4); Zn−O(10) 2.219(3).

various conformational structures. The substituent on the bridging nitrogen imposed most probably the steric effect on the formation of conjugation systems.

Conclusion

In summary, we have developed an efficient method for the synthesis of all $(NH)_m(NMe)_{4-m}$-bridged calix[4]pyridines **19**−**23** from deprotection of *N*-allyl groups of $(NAllyl)_m(NMe)_{4-m}$-bridged calix[4]pyridine derivatives **8** and **15**−**18**, which were prepared by macrocyclic coupling reaction between simple fragments. $(NH)_m(NMe)_{4-m}$-bridged calix[4]pyridines adopted different 1,3-alternate conformations in the solid state mainly due to the formation of varied conjugation systems of bridging NH units with their neighboring pyridines. In solution, all $(NH)_m$-$(NMe)_{4-m}$-bridged calix[4]pyridines were very fluxional and the rates of interconversion of various conformational structures might be very rapid relative to the NMR time scale, because of the lack of steric hindrance and intramolecular hydrogen bonds. Among all $(NH)_m(NMe)_{4-m}$-bridged calix[4]pyridines prepared, $(NH)_4$-bridged calix[4]pyridine **23** formed the strongest conjugation system. While $(NH)_m(NMe)_{4-m}$-bridged calix[4]pyridines, multi-nitrogen-containing macrocyclic host molecules, were able to form a 1:1 complex with metal ions, $(NH)_2(NMe)_2$-bridged calix-[4]pyridine **21** acted as a selective probe in the recognition of zinc(II) ion in solution with the dramatic enhancement of fluorescence intensity. The relatively easy availability, interesting structural and molecular recognition properties, and amenability to further modifications and functionalizations on the bridging NH units would render $(NH)_m(NMe)_{4-m}$-bridged calix[4]pyridines the macrocyclic host molecules useful in supramolecular chemistry.

Experimental Section

General Procedure for the Synthesis of $(NAllyl)_m(NMe)_{4-m}$-Bridged Calix[4]pyridines 8 and 15−18. Under argon protection, a mixture of diamine (2 mmol) and dibromide (2.2 mmol), $Pd_2(dba)_3$ (184 mg, 0.2 mmol), dppp (164 mg, 0.4 mmol), and sodium *tert*-butoxide (576 mg, 6 mmol) in anhydrous toluene (400 mL) was refluxed for 5 h. The reaction mixture was cooled to room temperature and filtered through a Celite pad. The filtrate was concentrated under vacuum to remove toluene and the residue was dissolved in dichloromethane (50 mL) and washed with brine (3 × 15 mL). The aqueous phase was re-extracted with dichloromethane (3 × 20 mL). The combined organic phase was dried over anhydrous Na_2SO_4. After removal of solvent, the residue was chromatographed on a silica gel column (100−200) with a mixture of petroleum ether and acetone as the mobile phase to give the products.

$(NAllyl)_4$-Bridged Calix[4]pyridine 18: white solid; mp 149−150 °C; ^{1}H NMR (300 MHz, $CDCl_3$) δ 7.34−7.29 (m, 4H), 6.38−6.34 (m, 8H), 5.91−5.86 (m, 4H), 5.31−5.25 (m, 4H), 5.10−5.06 (m, 4H), 4.52−4.46 (m, 4H), 4.06−4.00 (m, 4H); ^{13}C NMR (75 MHz, $CDCl_3$) δ 158.4, 138.4, 135.2, 115.3, 109.2, 52.2; IR (KBr) ν 1572 cm^{-1}; MS (MALDI-TOF) m/z 529 $[M + H]^+$ (100), 551 $[M + Na]^+$ (7). Anal. Calcd for $C_{32}H_{32}N_8$: C, 72.70; H, 6.10; N, 21.20. Found: C, 72.83; H, 6.25; N, 21.10.

General Procedure for the Synthesis of $(NH)_m(NMe)_{4-m}$-Bridged Calix[4]pyridines 19−23. Under argon protection, a mixture of $(NAllyl)_m(NMe)_{4-m}$-bridged calix[4]pyridines (m = 1−4) and potassium *tert*-butoxide (1.5−6 equiv) in anhydrous DMSO (20 mL) was heated at 100 °C for 1 h. The reaction mixture was cooled to room temperature, and dichloromethane (50 mL) and water (50 mL) were added. The organic layer was separated, and the aqueous layer was extracted with dichloromethane (2 × 25 mL). The combined organic layers were washed with water. After removal of solvent, the residue was dissolved in 20 mL of a mixture of acetone and water (9:1), acidified with concentrated hydrochloric acid (10−40 equiv). The resulting mixture was then refluxed for 1 h. After removal of solvent, the residue was worked up by two methods. Method A: The residue was dissolved in dichloromethane (100 mL) and washed with saturated Na_2CO_3 solution (50 mL), and aqueous phase was re-extracted with dichloromethane (2 × 50 mL). The combined organic phase was washed with brine (2 × 50 mL) and dried over anhydrous Na_2SO_4. After removal of solvent, the residue was chromatographed on a basic aluminum oxide column with a mixture of petroleum ether and acetone as the mobile phase to give the products. Method B: The residue was dissolved in methanol (50 mL) and water (50 mL), then adjusted to pH 10 with saturated Na_2CO_3 solution. After removal of solvent, the residue was washed with water and dried by vacuum, then purified by recrystallization with acetone to give the product.

$(NH)_4$-Bridged Calix[pyridine 23: white solid; mp 297−298 °C; ^{1}H NMR (300 MHz, CD_3COCD_3) δ 7.58 (br s, 4H), 7.34 (t, J = 7.8 Hz, 4H), 6.33 (d, J = 7.8 Hz, 4H); ^{13}C NMR (75 MHz, CD_3COCD_3) δ 156.5, 139.0, 108.2; IR (KBr) ν 3399, 3274, 1615, 1574 cm^{-1}; MS (MALDI-TOF) m/z 369 $[M + H]^+$

(100), 391 $[M + Na]^+$ (25); exact mass (HRESI) found 369.15680, $C_{20}H_{17}N_8$ requires 369.15707.

Acknowledgment. We thank the National Natural Science Foundation of China, Ministry of Science and Technology (2007CB808005), and Chinese Academy of Sciences for financial support.

Supporting Information Available: Experimental details and characterizations of products, ^1H and ^{13}C NMR spectra of products, UV−vis and fluorescence spectra of products, fluorescence titration spectra, cyclic voltammetric curves, X-ray structure of **19**−**23** and **23**-$Zn(ClO_4)_2$ complex (CIF). This material is available free of charge via the Internet at http://pubs.acs.org.